Eur J Nucl Med Mol Imaging (2015) 42:1767–1777
DOI 10.1007/s00259-015-3138-y

GUIDELINES

^{18}F-NaF PET/CT: EANM procedure guidelines for bone imaging

M. Beheshti[1] · F. M. Mottaghy[2,3] · F. Payche[4] · F. F. F. Behrendt[2] · T. Van den Wyngaert[5] · I. Fogelman[6] · K. Strobel[7] · M. Celli[8] · S. Fanti[8] · F. Giammarile[9] · B. Krause[10] · W. Langsteger[1]

Received: 6 July 2015 / Accepted: 8 July 2015 / Published online: 23 July 2015

Abstract The aim of this guideline is to provide minimum standards for the performance and interpretation of ^{18}F-NaF PET/CT scans. Standard acquisition and interpretation of nuclear imaging modalities will help to provide consistent data acquisition and numeric values between different platforms and institutes and to promote the use of PET/CT modality as an established diagnostic modality in routine clinical practice. This will also improve the value of scientific work and its contribution to evidence-based medicine.

Keywords Guideline · F-18 sodium fluoride · PET/CT · Bone imaging

Preamble

This practice guideline is an educational tool designed to help advance the knowledge regarding ^{18}F-NaF PET/CT imaging and to improve the quality of service to patients throughout Europe. It represents a policy statement by the European Association of Nuclear Medicine (EANM) and has been subjected to extensive review, requiring the approval of oncology and bone and joint committees, as well as the directory board of EANM.

The practice guidelines assist practitioners to follow a reasonable course of action based on current knowledge in providing effective and safe medical care for patients. They are not intended to establish a legal standard of care. Thus, the final decision regarding the appropriateness, indication, and priority of any specific medical procedure must be made based on reasonable judgment of the physician in light of the condition of the patient, limitations of available resources, advances in knowledge, and consequence of the course of action.

Introduction

^{18}F Sodium Fluoride (^{18}F-NaF) is a positron-emitting, bone seeking, radiopharmaceutical that was used briefly for skeletal scintigraphy in the 1970s [1–3]. However, its clinical use was

✉ M. Beheshti
mohsen.beheshti@bhs.at

1 PET - CT Center LINZ, Department of Nuclear Medicine & Endocrinology, St Vincent's Hospital, Seilerstaette 4, A-4020 Linz, Austria

2 Department of Nuclear Medicine, University Hospital Aachen, RWTH Aachen University, Aachen, Germany

3 Department of Nuclear Medicine, Maastricht University Medical Center, Maastricht, The Netherlands

4 Department of Nuclear Medicine, Louis Mourier Hospital, Colombes, Cedex, France

5 Department of Nuclear Medicine, Antwerp University Hospital, Edegem, Belgium

6 Department of Nuclear Medicine, Guy's Campus, King' College, London, UK

7 Department of Radiology and Nuclear Medicine, Lucerne Cantonal Hospital, Lucerne, Switzerland

8 Department of Nuclear Medicine, PET Unit, Policlinico S. Orsola-Malpighi, Bologna, Italy

9 Department of Nuclear Medicine, Centre Hospitalier Universitaire de Lyon, Lyon, France

10 Department of Nuclear Medicine, University Hospital Rostock, Rostock, Germany

limited at that time mainly due to its high 511 keV energy annihilation photons, the logistic difficulties in delivering a tracer with short half-life of 110 min, as well as due to the less than ideal features of conventional gamma cameras. With the advent of the first technetium-99 m (^{99m}Tc) based phosphonates in the late 1970s and the development of the Anger camera, ^{18}F-NaF was largely replaced by ^{99m}Tc-labeled phosphonates that have optimal characteristics for conventional gamma cameras [2, 3].

During the last few decades, bone scintigraphy has been used routinely in the assessment of malignant and benign diseases in the skeleton. However, it shows limited sensitivity and specificity. The advent of single photon emission tomography (SPECT) in particular in combination with computed tomography (CT) has further increased the diagnostic accuracy of planar bone scintigraphy and its clinical applications [4, 5]. Increasing implementation of PET/CT devices and use of ^{18}F labeled agents in the last few years has rekindled the interest in using ^{18}F-NaF.

Common standards will help consistent data acquisition and numeric values between different platforms and institutes to promote the use of PET/CT modality and optimal imaging that would be acceptable by any clinician in any institute. This will also increase the value of scientific work and its contribution to evidence-based medicine which is necessary for optimal patient management and standard health care in different hospitals. This guideline will, therefore, provide general information about ^{18}F-NaF PET/CT to assist physicians to carry out, interpret, and document ^{18}F-NaF PET/CT studies and to standardize diagnostic quality and quantitative information.

Principle and definitions

See European Association of Nuclear Medicine procedure guidelines for tumour PET imaging [6] and the Society of Nuclear Medicine practice guideline for ^{18}F-NaF PET/CT bone scan 1.0 [7].

Preparation

^{18}F-NaF is produced by 11-MeV proton irradiation of ^{18}O-water in a tantalum target body (10) using a cyclotron. The irradiated aqueous solution containing ^{18}F-NaF is diluted with sterile water (5 mL) and passed through a cation exchange (H^+ form) cartridge. The eluent from the cation exchange cartridge is passed through an anion exchange ($HCO3^-$ form) cartridge to trap the ^{18}F NaF. The anion exchange cartridge is then flushed with 10 mL of sterile water, and the 18 F fluoride is then eluted with 10 mL of sterile normal saline and is passed through a sterile filter into a sterile multidose vial [2]. The quality control tests for the ^{18}F-NaF conform to the European Pharmacopeia.

Pharmacokinetics and uptake mechanism

PET with the short half-life bone seeking agent ^{18}F-NaF ($T_{1/2}$=110 min) provide a unique way of assessment of regional bone metabolism that complements other investigations such as bone biopsy and biochemical markers as an assistant tool for research studies [8, 9]. ^{18}F-NaF binds to sites of new bone formation and serves as a marker of bone blood flow and osteoblastic activity [10–12]. Bone is composed of two thirds mineral and one third collagen, an extracellular matrix, and a variety of bone lining cells. The mineral matrix is composed of calcium hydroxyapatite. Uptake of ^{18}F-NaF has a similar mechanism to ^{99m}Tc-MDP. Following chemisorption of fluoride ions onto the surface of hydroxyapatite, they exchange with the hydroxyl (OH^-) ions in the crystal, forming fluoroapatite [13].

$$Ca_5(PO_4)_3OH + F^- \rightarrow Ca_5(PO_4)_3F + OH^-$$

^{18}F-NaF undergoes rapid blood clearance with first-pass clearance close to 100 % [14] mainly due to a negligible proportion of protein binding. Plasma clearance is very rapid, and only 10 % of ^{18}F-NaF remains in the plasma in about 1 h after injection [2], and the 5 h integrated plasma concentration was only 1.1–2.6 % of the dose per liter. The reported 5 h cumulative urine excretion was 7.4–24.8 % in eight patients [2, 15]. Approximately 50 % of the injected ^{18}F-NaF is taken up in bone [3] and about 30 % of the injected dose is in red blood cells, which does not interfere with bone uptake as ^{18}F-NaF freely diffuses across the cell membrane [2]. The remainder excreted by the kidneys by 6 h after tracer administration. These properties permit a short uptake time of ^{18}F-NaF allowing early imaging acquisition.

Moreover, quantitative ^{18}F-NaF PET imaging provides a novel way to study bone metabolism as an additional research tool besides conventional measurements using bone turnover markers in the investigation of new treatments for osteoporosis. The advantage of ^{18}F-NaF PET to bone markers that measure the integrated response to treatment across the whole skeleton is to distinguish the changes occurring at sites of particular clinical interest such as the hip and spine [16, 17]. Dynamic PET imaging can be used to measure the effective bone plasma flow (K_1, from which bone blood flow can be estimated) and the fluoride plasma clearance to bone mineral (K_i) at sites within the field of view of the PET scanner. Following completion of the dynamic scan, a series of static scan images can be used to estimate K_i at any number of additional sites throughout the skeleton provided between two and four venous blood samples are taken to derive the input function.

Standardised uptake values (SUVs) in bone can also be measured [18].

Indications

PET is an evolving diagnostic imaging modality with occasional differences in indications between individual countries depending on their health care systems.

The Centers for Medicare and Medicaid Services (CMS) issued a decision memorandum regarding the use of ^{18}F-NaF PET for detection of bony metastasis in February 26, 2010, that "the available evidence is sufficient to determine that ^{18}F-NaF PET imaging to identify bone metastasis of cancer to inform the initial antitumor treatment strategy or to guide subsequent antitumor treatment strategy after the completion of initial treatment, is reasonable and necessary"; however, the CMS has concluded that the evidence is not sufficient to determine that the results of ^{18}F-NaF PET imaging to identify bone metastases improved health outcomes of beneficiaries with cancer, and therefore, this use is not reasonable and necessary under the Social Security Act [19]. This resulted in the creation of the National Oncologic PET Registry for ^{18}F-NaF (NOPR ^{18}F-NaF PET) [20–22]. The initial results of NOPR in prostate cancer patients showed that the post imaging plan was revised to treatment in 77 % of patients referred for initial staging. The authors reported a high overall impact of ^{18}F-NaF PET, principally related to its effect on replacing intended use of other advanced imaging. Its imaging adjusted impact was similar to that observed with ^{18}F-FDG PET for restaging or suspected recurrence in other cancer types [21].

In non-prostate cancer patients ^{18}F-NaF PET led to change in intended management in a substantial fraction of patients [22].

Conventional ^{99m}Tc-MDP bone scintigraphy has been the method of choice for the assessment of bone metastases in cancers with various entities especially in prostate, lung, and breast cancers, since it provides a whole body survey with acceptable sensitivity at a relatively low cost [23, 24].

Applications of bone scintigraphy in the assessment of malignancies include initial staging, therapy monitoring and determining the areas at risk for pathological fracture. In addition, bone scintigraphy allows depicting various benign bone diseases such as metabolic and inflammatory bone diseases, as well as orthopedic disorders. In spite of the relative high sensitivity of ^{99m}Tc-MDP scintigraphy for the assessment of advanced bone metastases, it may have limited value in the detection of early bony involvement because this technique relies on the determination of the regional blood flow as well as osteoblastic activity of the bone lesions rather than the identification of the tumor itself. In addition, conventional planar scintigraphy showed limited spatial resolution for the detection of bone metastases in particular in complex skeletal structures such as spine, skull, and pelvis [25] that also affect its sensitivity [26]. Many studies show that single photon emission computed tomography (SPECT) can minimise the shortcomings of planar bone scintigraphy in the assessment of the spine [23, 27–34]. With development of the scanners capabilities, multi-field of view SPECT and SPECT/CT are proposed as superior methods compared to localized SPECT for the evaluation of bone metastases throughout the entire skeleton [35, 36].

Hence, the transition to the better resolution of PET/CT for assessment of bone metastases is demanding, with the use of the positron emitter ^{18}F-NaF as the radiotracer of choice. Recently, many studies have assessed the impact of PET or PET/CT in the assessment of bone metastases with the use of the positron emitter ^{18}F-NaF as the radiotracer of choice [35–40]. They showed that ^{18}F-NaF PET is more accurate than ^{99m}Tc-MDP planar imaging or SPECT for the assessment of malignant bone diseases. The higher-quality imaging, increased clinical accuracy, greater convenience to the patient and referring physician, and more efficient use of nuclear medicine resources all indicate the need to reconsider the use of ^{18}F-NaF PET for imaging malignant skeletal diseases [37]. Despite the high performance of ^{18}F-NaF PET/CT, its clinical use remains limited because of the still-limited availability of PET/CT scanners when compared with gamma cameras, lack of uniform reimbursements, and lack of standard validated interpretation criteria.

The main clinical indications of ^{18}F-NaF PET/CT are identification of bone metastases, correct determination of the extent of disease, and localization of the malignant bony lesions [24, 35, 37, 41–46]. However, based on current data, the following indications have been suggested to be appropriate in certain cases:

Benign bone disease

- Metabolic bone disease and assessment of the therapy [47]
- Osteomyelitis
- Spondyloarthropathies, axial and/or peripheral forms [48, 49]
- Osteoarthritis (hip, knee, foot) [50, 51]
- Avascular osteonecrosis [52–55]
- Paget's disease [56]
- Foot pain of unclear origin [57]
- Unexplained pain syndrome

Orthopedic applications

- Heterotopic ossification

- Complex regional pain syndrome
- Painful prosthetic joints [58, 59]
- Trauma and overuse injuries [60]
- Occult (stress) fractures
- Insufficiency fractures
- Spondylolysis and spondylolisthesis
- Enthesopathies
- Viability of Bone grafts [61]

Malignant bone disease

- Primary bone malignancies [62]
- Metastatic bone disease and evaluation of the treatment response
- Abnormal radiographic or laboratory findings

Pediatric bone diseases [46]

- Bone Trauma, child abuse [63]
- Back pain [48, 64]
- Osteochondrosis and condylar hyperplasia [65]
- Osteoid osteoma [46]
- Langerhans cell histiocytosis [46]

Necessary data for requesting ^{18}F-NaF PET/CT

Requisition for ^{18}F-NaF PET/CT by the referring physician should ideally be accompanied by a concise summary of the patient's history with a relevant clinical question.

- Indication, reason for requesting ^{18}F-NaF PET/CT
- Height and body weight (if semi-quantitative measurement by SUV is required). Weight must be measured directly prior to each PET study as body weight may not be constant during the course of disease
- History of malignancy (if known, tumor type and site)
- Oncology prior history (date of type of previous therapeutic intervention, e.g., chemo- and/or radiotherapy)
- Previous fractures or recent trauma (date and site of injury)
- Previous orthopedic surgery and relevant dates (date, type, and site of intervention)
- Previous infection and its location
- Urinary diversion procedures
- Location of any bone pain
- The results of other imaging modalities (especially bone scan, CT, or MRI).

Patient preparation

The patients should be fully informed about the concept and technical performance of the examination. Principally, ^{18}F-NaF PET/CT has the same preparation as bone scintigraphy [7, 66] (see also the EANM practice guideline for bone scintigraphy 2014).

- Regarding pregnant or breastfeeding patients, see Section VI of the SNM Procedure Guideline for General Imaging or national guidelines. Examinations involving ionizing radiation should be avoided in pregnant women, unless the potential benefits outweigh the radiation risk to the mother and fetus.
- Patients should be well hydrated before the study and during the uptake time [at least two glasses (about 450 mL) of water] in order to enhance renal excretion, reducing radiation exposure and achieving optimal target to background ratio. Patients are also encouraged to drink more frequently for the remainder of the day.
- Patients should be asked to empty their bladders before image acquisition.
- Any metal objects should be removed to prevent attenuation artefacts.
- Patients do not need to fast and are allowed to take all their usual medications.

Dosage of radioactivity

^{18}F-NaF is injected intravenously by direct venipuncture or intravenous catheter as follows:

- Adults: 1.5–3.7 MBq /kg; a maximum recommended dose (370 MBq) should be considered for obese patients.
- Pediatrics: 2.2 MBq/kg is administered with a minimum activity of 18.5 MBq and the maximum level not exceeding 185 MBq.

High administered doses (which do not result in improved diagnostic sensitivity or accuracy) or low doses (which do not permit an adequate imaging examination) should be considered unnecessary radiation exposures. Dose estimations for pediatric patients that are based on adult dose corrected for body weight are generally reasonable guides for children older than 1 year of age. Premature infants and newborns require special consideration, and minimum total doses may be used. *Minimum total dose* can be defined as the minimum dose of radiopharmaceutical administered activity below which the study may likely be inadequate, regardless of the patient's body weight [67].

Oral administration of ^{18}F-NaF has been performed previously. Because of rapid and complete intestinal absorption of ^{18}F-NaF, its image quality seems to be comparable with intravenous administration. However, incomplete absorption of ^{18}F-NaF in some patients may cause increased tracer uptake in the gastrointestinal tract [68], which seems not to affect the diagnostic accuracy of this modality when using current hybrid PET/CT devices. This route of administration may represent an alternative to intravenous injection in patients with difficult venous access; however, this does not allow quantification.

Image acquisition

In patients with normal renal function, acquisition of the axial skeleton may begin about 30–45 min after administration of the radiopharmaceutical, due to prompt blood clearance and rapid skeletal uptake of ^{18}F-NaF. However, it is necessary to wait longer to obtain high-quality images of the extremities, with a start time of 90–120 min for imaging of the upper and lower extremities.

- For patient positioning see the EANM Procedure Guideline for Tumor Imaging with ^{18}F FDG PET/CT [6]. Arm position during scanning depends on the indications for the study. The arms may be by the sides for whole-body imaging or elevated when only the axial skeleton is scanned.
- PET images may be acquired in 2- or 3-dimensional mode. Three-dimensional mode is recommended for whole-body acquisition because the higher count rates compensate for the shorter acquisition times required for imaging a large area [7].
- Acquisition time per bed position will vary depending on the amount of injected radioactivity, uptake time, body mass index, body habitus of the patient, and camera factors. To obtain high-quality skeletal images on current devices, emission scans with acquisition times of 1–2 min per bed position in 3D mode are performed depending on the above mentioned parameters.
- Usually a 128×128 matrix will be applied for image acquisition, although a 256×256 matrix may be advantageous if processing times are reasonable. Commercially available software packages for iterative reconstruction are widely available. The optimal number of iterations and subsets, filters, and other reconstruction parameters will depend on patient and camera factors. In general, the same reconstruction protocols as are used for imaging ^{18}F-FDG PET may be used for ^{18}F-NaF. Maximum intensity projection images should be generated to help facilitate lesion detection.

Combination imaging with simultaneous ^{18}F-FDG and ^{18}F-NaF injection has been reported [69–71]; however, there is not sufficient data to support its use in routine clinical practice.

Whole-body CT of PET/CT imaging is acquired either immediately before or after the emission scan to provide CT based attenuation correction and anatomic localization. The CT protocol depends on the indications for the study and the likelihood that radiographic findings will add diagnostic information. The need for additional diagnostic information should always be weighed against the increased radiation exposure from CT. Dose parameters should be consistent with the principles of ALARA (as low as reasonably achievable).

The usual CT settings sufficient for attenuation correction and localization are a tube current of 30 mA, voltage of 120 kVp, rotation of 0.5 s, and pitch of 1.

Quantitative ^{18}F-NaF PET imaging

The Hawkins method

Quantitative ^{18}F-NaF PET studies are often performed using the dynamic scan method first described by Hawkins et al. [8]. This was the first radionuclide imaging technique to measure bone plasma clearance rather than bone uptake, and the method has since been widely adopted by other researchers [72–75]. The typical value of the ^{18}F-NaF plasma clearance to bone mineral in the lumbar spine is 0.03 mL min^{-1} mL^{-1} (e.g., the amount of tracer taken up in one millilitre of bone tissue in 1 min is the same as that transported in 0.03 mL of plasma) [18, 76]. The protocol of quantitative ^{18}F-NaF PET imaging is shown in Table 1.

In the Hawkins method, the subject receives a bolus injection of ^{18}F-NaF in a 10-mL saline solution, and simultaneously a 60-min dynamic PET scan is acquired, imaging the chosen site in the skeleton. A set of protocols for image acquisition and reconstruction are summarised in Table 1 [76]. The bone ROIs are restricted to the 15-cm section of the human body that can be included in the field of view of the PET scanner, for example, the lumbar spine (L1-L4) or the hip. To measure bone plasma clearance, it is also necessary to obtain the arterial input function (aIF), and this can be done either by direct monitoring using an arterial blood line [8, 56, 74, 75] by using an image derived input function from an ROI placed over the abdominal aorta,[36] or by using a population derived curve calibrated against venous blood samples obtained 30 to 60 min after injection.[73]

The object of the dynamic PET scan is to obtain the time-activity curves (TAC) for the concentration of ^{18}F-NaF in the bone ROI and arterial blood during the first 60 min following the bolus injection. Both curves are corrected for radioactive decay of ^{18}F back to the time of injection. These curves are

Table 1 Protocols for quantitative PET image acquisition and reconstruction [57]

Acquisition	60-min dynamic study on PET/CT scanner
Scan mode	2D or 3D
Frame times:	24×5 s. 4×30 s. 14×240 s.
Patient preparation:	Patient should be well hydrated and comfortable on scan table
CT scout scan:	10 mA at 120 kVp
Patient positioning:	Spine: L1-L4 including bottom of T12 and top of L5 Hip: 1 cm above acetabulum to mid femoral shaft
Injected activity:	90 MBq (lumbar spine) or 180 MBq (hip) ^{18}F-NaF in 10 mL saline
Injection protocol:	T0: Start dynamic scan T0+10 s: Start injection of ^{18}F-NaF T0+20 s: Finish injection. Follow with 10 mL saline flush T0+30 s: Finish saline flush
Blood sampling (for semi-population arterial input function)	Venous blood samples (1.5 mL) from opposite arm to injection at 30, 40, 50, and 60 min
Reconstruction parameters:	Matrix size: 128×128 Reconstruction: Filtered back projection Attenuation correction: From CT image Transaxial filter: Hanning 6.3 mm Random correction: Correction from singles Deadtime correction: Yes Scatter correction: Yes

then analysed using the compartmental model (the Hawkins model) shown in Fig. 1 to find the effective bone plasma flow to bone tissue (K_1) and the plasma clearance to the bone mineral compartment (K_i) [8]. In the Hawkins model the rate constant K_1 describes the clearance of ^{18}F-NaF from plasma to the unbound bone pool, k_2 the reverse transport from the unbound bone pool back to plasma, k_3 the forward transport from the unbound bone pool to bone mineral, and k_4 the reverse flow. Bone blood flow can be estimated from K_1 knowing the packed cell volume and the first pass extraction of ^{18}F-NaF, which is often assumed to be 100 % [77, 78]. The parameter K_i representing the plasma clearance of ^{18}F-NaF to bone mineral is calculated from the following equation [8, 76]:

$$K_i = K_1 x k_3/(k_2 + k_3)\ \text{mL min}^{-1}\text{mL}^{-1} \quad (1)$$

In Eq. (1) the ratio k_3 / (k_2+k_3) represents the fraction of tracer initially cleared to bone tissue that binds to bone mineral and takes values between 0 and 1.0. The use of K_i to study bone formation was validated in two reports that found correlations with histomorphometric indices of bone formation and mineral apposition rate [12]. Alternative methods to the Hawkins model for analysing the bone TAC and IF curves to evaluate K_1 and K_i include deconvolution and spectral analysis [79]. A fourth method, the Patlak plot, provides a simple graphical method of evaluating K_i, but cannot be used to find K_1 [79].

Standardised uptake values

A simpler method of quantifying PET studies that avoids the need to find the input function is to measure standardised uptake values (SUVs) by normalising the mean ^{18}F-NaF concentration in the bone region of interest for injected activity and body weight [SUV_{mean}=Mean kBq/mL x Body Weight (kg)/Injected Activity (MBq)]. In PET studies that image malignant disease it is common to evaluate mean or peak values of SUV, and this practice can be justified on the grounds of the frequent lack of homogeneity of tracer uptake seen in tumours [80]. However, SUV measurement is not routinely used in interpretation of ^{18}F-NaF PET/CT studies. In addition, in osteoporosis and other types of diffuse metabolic bone disease, the ^{18}F-NaF uptake in bone tissue such as the vertebral body or the femoral shaft is quite uniform, and so the mean SUV within the bone ROI is a more appropriate index than the maximum value. It is important to mention that accurate quantitative analysis warrants standard scanner calibration, acquisition parameters as well as image reconstruction.

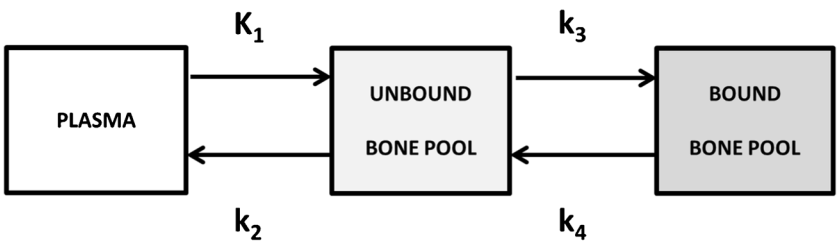

Fig. 1 The Hawkins compartmental model [8] used for the analysis of ^{18}F-NaF PET dynamic bone scans. The rate constant K_1 describes the effective bone plasma flow to the unbound bone pool, k_2 the reverse transport of tracer from the unbound bone pool back to plasma, k_3 the forward transport from the unbound bone pool to bone mineral, and k_4 the reverse flow

One disadvantage of the Hawkins method is that with a single injection of ^{18}F-NaF it is only possible to perform a single 60-min dynamic scan at one chosen site in the skeleton [76]. Therefore, the measurements are restricted to the 15-cm field of view of the PET scanner. In contrast, SUV measurements have the advantage that they require only a short (2–5 min.) static scan at the measurement site compared with the 60-min scan required by the Hawkins method. Hence, with a series of static scans starting 30–40 min after injection it is possible to measure SUVs over most of the skeleton during a period when the bone time-activity curve is only slowly changing [76].

To date, only a few studies have assessed SUV impact on the reporting of ^{18}F-NaF PET/CT because it is not routinely used in interpretation of the bone studies. One study measured the SUVmax of ^{18}F-NaF uptake in metastatic lesions in a variety of malignancies. Sclerotic or mixed lesions had higher SUV values than lytic sites. The same was found for lesions involving both the cortex and medulla when compared to those involving only the cortex or the medulla [81]. In a study comparing ^{18}F-NaF to F-18 fluorocholine (FCH) PET/CT in patients with prostate cancer, SUVmax was measured in all bone metastases [82]. With ^{18}F-NaF, mean SUVmax in malignant lesions was considerably higher comparing to benign lesions. The applicability of this statement in routine clinical work is however questionable as certain benign bone entities including fibrous dysplasia, Paget's disease and acute fractures can demonstrate very intense uptake [46]. Interval changes in SUVmax have been found in a small number of patients to be able to predict response to therapy, even in the absence of differences on visual comparison [83].

Radiation dosimetry

The effective dose to the patient from an injection of 370 MBq of ^{18}F-NaF is about 8.9 mSv compared to 4.2 mSv for 740 MBq of ^{99m}Tc-MDP for SPECT [71]. However, considering higher sensitivity and diagnostic accuracy of new PET/CT scanners which provide high quality images with lower tracer activity (i.e., 2.0 MBq/kg), the radiation burden of ^{18}F-NaF PET/CT seems to be similar or even less than ^{99m}Tc-MDP scan depending on the applied activity and CT acquisition parameters. A meta-analysis reported a range of values of 2.7 to 15.0 mSv for ^{18}F-NaF versus 4.2 to 5.7 mSv for ^{99m} Tc-MDP, respectively [84]. In children, these values are lower [48]. The radiation exposure associated with the CT component of PET/CT and SPECT/CT studies is highly variable and ranges from less than 1 mSv for CT-attenuation correction only [85], to about 8 mSv for a diagnostic CT scan [86]. A typical value for an effective low-dose CT used for localization and attenuation correction is 3.2 mSv [7]. Consequently, the total effective dose of ^{18}F-NaF PET with a low-dose CT bone scan is approximately 12.1 mSv compared to approximately 7.4 mSv for a bone SPECT/CT. The radiation dosimetry of ^{99m}Tc-MDP bone scintigraphy versus ^{18}F-NaF PET is shown in Table 2.

Normal biodistribution and image interpretation

See also EANM Procedure Guideline for conventional bone scintigraphy 2014.

In general, normal ^{18}F-NaF PET demonstrates uniform tracer distribution throughout the skeleton. The pattern of physiologic tracer uptake may also be slightly non-homogeneous which reflects differences in regional blood flow as well as differences in the bone crystal surface area accessible to the tracer [68]. Normal growth causes increased tracer uptake in the metaphyses of children and adolescents. Normal ^{18}F-NaF shows generally a symmetrical tracer uptake except peri-articular regions that may show variable pattern of tracer uptake. Normal urinary washout is the major route of tracer excretion which leads to kidney, ureters, and urinary bladder visualization if renal function is within the normal limits. However, the degree of tracer accumulation in the urinary tract depends on the renal function, state of hydration and interval between tracer administration and acquisition [7]. Bone to soft tissue contrast reflects the amount of ^{18}F-NaF in blood pool at the time of imaging. Hyperemia may cause local or regional increased of soft tissue uptake.

Any causes of altered bone metabolism may cause increased ^{18}F-NaF uptake which is mainly dependent on regional blood flow and/or new bone formation. Lesions with minimal osteoblastic bone changes, or mainly osteolytic changes may show different patterns from undetectable to activity only at the rim of periphery of a lesion or even markedly increased tracer uptake [42, 87]. ^{18}F-NaF uptake may be quite prominent in benign findings as well. Therefore, the degree of ^{18}F-NaF uptake cannot differentiate benign from malignant lesions. Nevertheless, the pattern of tracer uptake may be suggestive or rather characteristic of a specific diagnosis [7]. The CT component of PET/CT, even when performed for attenuation correction and localisation, potentially improves the interpretation. For those who are routinely reading conventional bone scans, a learning curve is associated with the interpretation of ^{18}F-NaF PET/CT prior to becoming familiar with the normal and sometimes prominent heterogeneity of tracer distribution.

Table 2 Radiation dosimetry of ^{99m}Tc MDP bone scintigraphy versus ^{18}F-NaF PET [88, 89]

Tracer	Adult (70 kg)	15 years (55 kg)	10 years (32 kg)	5 years (19 kg)	1 year (9.8 kg)
^{99}mTc-MDP					
Administered activity (MBq)	518	407	237	141	73
Effective dose in mSv/MBq (mSv)	0.0057 (3.0)	0.0070 (2.8)	0.0110 (2.6)	0.0140 (2.0)	0.0270 (2.0)
Bladder wall in mGy/MBq (mGy)	0.048 (24.9)	0.060 (24.4)	0.088 (20.9)	0.073 (10.3)	0.130 (9.5)
Bone surfaces (mGy)	0.063 (32.6)	0.082 (33.4)	0.130 (30.8)	0.220 (31.0)	0.53 (38.7)
Red marrow (mGy)	0.0092 (4.8)	0.010 (4.1)	0.017 (4.0)	0.033 (4.7)	0.067 (4.9)
^{18}F-NaF					
Administered activity (MBq)	148	116	68	40	21
Effective dose in mSv/MBq (mSv)	0.027 (4.0)	0.034 (3.9)	0.052 (3.5)	0.086 (3.4)	0.170 (3.6)
Bladder wall in mGy/MBq (mGy)	0.22 (32.6)	0.27 (31.3)	0.40 (27.2)	0.61 (24.4)	1.10 (23.1)
Bone surfaces in mGy/MBq (mGy)	0.040 (5.9)	0.050 (5.8)	0.079 (5.4)	0.130 (5.2)	0.300 (6.3)
Red marrow in mGy/MBq (mGy)	0.040 (5.9)	0.053 (6.1)	0.088 (6.0)	0.180 (7.2)	0.380 (8.0)

Values in parentheses are doses in mGy (mSv for effective dose) for administered activity listed in table for that patient size

Documentation and reporting

See Society of Nuclear Medicine Guideline for ^{18}F-NaF PET/CT bone scans 1.0 [7] and European Association of Nuclear Medicine procedure guidelines for tumour PET imaging [6].

General aspects

1. Document the appropriateness, necessity, performance, and quality of the procedure
2. Timely response to the clinical question within the limits of the examination
3. Findings likely to have a significant, immediate influence on patient care should be communicated to the requesting physician or an appropriate representative in a timely manner.
4. All actual or tried communications should be documented as appropriate.
5. Significant discrepancies between an initial and final report should be directly communicated, reconciled, and documented.
6. Expedite and assure correct billing

Contents of the report

See also EANM guidelines for FDG PET and PET/CT imaging.

The report should provide:

1. Study identification
2. Clinical information
3. Procedure description
4. Findings description (including clinical findings and quality of exam)
5. Conclusion and comment

Equipment specification, quality control

See "equipment specification" and "quality control" of FDG PET and PET/CT imaging: EANM procedure guidelines for tumor imaging.

Radiation safety

In all patients, the lowest exposure parameters to obtain the appropriate diagnostic quality should be selected.

The effective dose for ^{18}F-NaF is 0.024 mSv/MBq compared to 0.0057 mSv/MBq for ^{99m}Tc-MDP. The radiation dose to patients is about twice as high as using ^{18}F-NaF for a typical activity of 370 MBq ^{18}F-NaF and 740 MBq ^{99m}Tc-MDP (i.e., 8.9 mSv vs. 4.2 mSv, respectively).

No recommendation is provided concerning interruption of breastfeeding for ^{18}F-NaF in the International Commission on Radiological Protection Publication 106, Appendix D [88]; however, the authors recommend that no interruption is needed for breastfeeding patients administered ^{99m}Tc-diphosphonates. Nevertheless, summary of product characteristics of the commercially available ^{99m}Tc-diphosphonates should be considered.

Acknowledgments The authors thank the EANM committees and national delegates for their critical review of the manuscript. Also, we appreciate the grate support of the EANM office in Vienna, especially Katharina Leissing during the development of this Guideline.

References

1. Blau M, Nagler W, Bender MA. Fluorine-18: a new isotope for bone scanning. J Nucl Med. 1962;3:332–4.
2. Czernin J, Satyamurthy N, Schiepers C. Molecular mechanisms of bone 18F-NaF deposition. J Nucl Med. 51:1826–9. doi: 10.2967/jnumed.110.077933.
3. Grant FD, Fahey FH, Packard AB, Davis RT, Alavi A, Treves ST. Skeletal PET with 18F-fluoride: applying new technology to an old tracer. J Nucl Med. 2008;49:68–78. doi:10.2967/jnumed.106.037200.
4. Beheshti M, Langsteger W, Fogelman I. Prostate cancer: role of SPECT and PET in imaging bone metastases. Semin Nucl Med. 2009;39:396–407. doi:10.1053/j.semnuclmed.2009.05.003.
5. Ben-Haim S, Israel O. Breast cancer: role of SPECT and PET in imaging bone metastases. Semin Nucl Med. 2009;39:408–15. doi: 10.1053/j.semnuclmed.2009.05.002.
6. Boellaard R, Delgado-Bolton R, Oyen WJ, Giammarile F, Tatsch K, Eschner W, et al. FDG PET/CT: EANM procedure guidelines for tumour imaging: version 2.0. Eur J Nucl Med Mol Imaging. 2015;42:328–54. doi:10.1007/s00259-014-2961-x.
7. Segall G, Delbeke D, Stabin MG, Even-Sapir E, Fair J, Sajdak R, et al. SNM practice guideline for sodium 18F-fluoride PET/CT bone scans 1.0. J Nucl Med. 51:1813–20. doi: 10.2967/jnumed.110.082263.
8. Hawkins RA, Choi Y, Huang SC, Hoh CK, Dahlbom M, Schiepers C, et al. Evaluation of the skeletal kinetics of fluorine-18-fluoride ion with PET. J Nucl Med. 1992;33:633–42.
9. Moore AE, Blake GM, Taylor KA, Ruff VA, Rana AE, Wan X, et al. Changes observed in radionuclide bone scans during and after teriparatide treatment for osteoporosis. Eur J Nucl Med Mol Imaging. 39:326-36. doi:10.1007/s00259-011-1974-y.
10. Blake GM, Park-Holohan SJ, Cook GJ, Fogelman I. Quantitative studies of bone with the use of 18F-fluoride and 99mTc-methylene diphosphonate. Semin Nucl Med. 2001;31:28–49.
11. Messa C, Goodman WG, Hoh CK, Choi Y, Nissenson AR, Salusky IB, et al. Bone metabolic activity measured with positron emission tomography and [18F]fluoride ion in renal osteodystrophy: correlation with bone histomorphometry. J Clin Endocrinol Metab. 1993;77:949–55.
12. Piert M, Zittel TT, Becker GA, Jahn M, Stahlschmidt A, Maier G, et al. Assessment of porcine bone metabolism by dynamic. J Nucl Med. 2001;42:1091–100.
13. Fogelman I. Skeletal uptake of diphosphonate: a review. Eur J Nucl Med. 1980;5:473–6.
14. Wootton RCD. The single-passage extraction of 18F in rabbit bone. Clin Phys Physiol Meas. 1966;7:333–43.
15. Weber DA, Greenberg EJ, Dimich A, Kenny PJ, Rothschild EO, Myers WP, et al. Kinetics of radionuclides used for bone studies. J Nucl Med. 1969;10:8–17.
16. Blake GM, Moore AE, Fogelman I. Quantitative studies of bone using (99m)Tc-methylene diphosphonate skeletal plasma clearance. Semin Nucl Med. 2009;39:369–79. doi:10.1053/j.semnuclmed.2009.05.001.
17. Blake GM, Siddique M, Frost ML, Moore AE, Fogelman I. Imaging of site specific bone turnover in osteoporosis using positron emission tomography. Curr Osteoporos Rep. 2014;12:475–85. doi:10.1007/s11914-014-0231-2.
18. Blake GM, Frost ML, Fogelman I. Quantitative radionuclide studies of bone. J Nucl Med. 2009;50:1747–50. doi:10.2967/jnumed.109.063263.
19. Centers for Medicare and Medicaid Services. National Coverage Determination (NCD) for Positron Emission Tomography (NaF-18) to Identify Bone Metastasis of Cancer. 2010;220.6.19.
20. NOPR. National Oncologic PET Registry. 2012.
21. Hillner BE, Siegel BA, Hanna L, Duan F, Shields AF, Quinn B, et al. Impact of 18F-Fluoride PET on intended management of patients with cancers other than prostate cancer: results from the national oncologic PET registry. J Nucl Med. 2014;55:1054–61. doi:10.2967/jnumed.113.135475.
22. Hillner BE, Siegel BA, Hanna L, Duan F, Shields AF, Coleman RE. Impact of 18F-fluoride PET in patients with known prostate cancer: initial results from the National Oncologic PET Registry. J Nucl Med. 2014;55:574–81. doi:10.2967/jnumed.113.130005.
23. Savelli G, Maffioli L, Maccauro M, De Deckere E, Bombardieri E. Bone scintigraphy and the added value of SPECT (single photon emission tomography) in detecting skeletal lesions. Q J Nucl Med. 2001;45:27–37.
24. Chan SC, Wang HM, Ng SH, Hsu CL, Lin YJ, Lin CY, et al. Utility of 18F-fluoride PET/CT and 18F-FDG PET/CT in the detection of bony metastases in heightened-risk head and neck cancer patients. J Nucl Med. 2012;53:1730–5. doi:10.2967/jnumed.112.104893.
25. Horger M, Bares R. The role of single-photon emission computed tomography/computed tomography in benign and malignant bone disease. Semin Nucl Med. 2006;36:286–94. doi:10.1053/j.semnuclmed.2006.05.001.
26. Even SE. Imaging of malignant bone involvement by morphologic, scintigraphic, and hybrid modalities. J Nucl Med. 2005;46:1356–67.
27. Coleman RE. Skeletal complications of malignancy. Cancer. 1997;80:1588–94. doi:10.1002/(SICI)1097-0142(19971015)80:8+<1588::AID-CNCR9>3.0.CO;2-G.
28. Han LJ, Au-Yong TK, Tong WC, Chu KS, Szeto LT, Wong CP. Comparison of bone single-photon emission tomography and planar imaging in the detection of vertebral metastases in patients with back pain. Eur J Nucl Med. 1998;25:635–8.
29. Kosuda S, Kaji T, Yokoyama H, Yokokawa T, Katayama M, Iriye T, et al. Does bone SPECT actually have lower sensitivity for detecting vertebral metastasis than MRI? J Nucl Med. 1996;37:975–8.
30. Savelli G, Chiti A, Grasselli G, Maccauro M, Rodari M, Bombardieri E. The role of bone SPET study in diagnosis of single vertebral metastases. Anticancer Res. 2000;20:1115–20.
31. Even-Sapir E, Martin RH, Barnes DC, Pringle CR, Iles SE, Mitchell MJ. Role of SPECT in differentiating malignant from benign lesions in the lower thoracic and lumbar vertebrae. Radiology. 1993;187:193–8.
32. Gates GF. SPECT bone scanning of the spine. Semin Nucl Med. 1998;28:78–94.
33. Jacobson AF, Fogelman I. Bone scanning in clinical oncology: does it have a future? Eur J Nucl Med. 1998;25:1219–23.
34. Uematsu T, Yuen S, Yukisawa S, Aramaki T, Morimoto N, Endo M, et al. Comparison of FDG PET and SPECT for detection of bone metastases in breast cancer. AJR Am J Roentgenol. 2005;184:1266–73.
35. Ota N, Kato K, Iwano S, Ito S, Abe S, Fujita N, et al. Comparison of (1)(8)F-fluoride PET/CT, (1)(8)F-FDG PET/CT and bone scintigraphy (planar and SPECT) in detection of bone metastases of differentiated thyroid cancer: a pilot study. Br J Radiol. 2014;87:20130444. doi:10.1259/bjr.20130444.
36. Palmedo H, Marx C, Ebert A, Kreft B, Ko Y, Turler A, et al. Whole-body SPECT/CT for bone scintigraphy: diagnostic value and effect on patient management in oncological patients. Eur J Nucl Med Mol Imaging. 2014;41:59–67. doi:10.1007/s00259-013-2532-6.
37. Even Sapir E, Metser U, Mishani E, Lievshitz G, Lerman H, Leibovitch I. The detection of bone metastases in patients with high-risk prostate cancer: 99mTc-MDP Planar bone scintigraphy, single- and multi-field-of-view SPECT, 18F-fluoride PET, and 18F-fluoride PET/CT. J Nucl Med. 2006;47:287–97.
38. Krger S, Buck A, Mottaghy F, Hasenkamp E, Pauls S, Schumann C, et al. Detection of bone metastases in patients with lung cancer:

99mTc-MDP planar bone scintigraphy, 18F-fluoride PET or 18F-FDG PET/CT. Eur J Nucl Med Mol Imaging. 2009;36:1807–12.
39. Schirrmeister H, Guhlmann A, Elsner K, Kotzerke J, Glatting G, Rentschler M, et al. Sensitivity in detecting osseous lesions depends on anatomic localization: planar bone scintigraphy versus 18F PET. J Nucl Med. 1999;40:1623–9.
40. Iagaru A, Mittra E, Dick D, Gambhir S. Prospective Evaluation of (99m)Tc MDP Scintigraphy, (18)F NaF PET/CT, and (18)F FDG PET/CT for Detection of Skeletal Metastases. Molecular imaging and biology. 2011.
41. Yen RF, Chen CY, Cheng MF, Wu YW, Shiau YC, Wu K, et al. The diagnostic and prognostic effectiveness of F-18 sodium fluoride PET-CT in detecting bone metastases for hepatocellular carcinoma patients. Nucl Med Commun. 2010;31:637–45. doi:10.1097/MNM.0b013e3283399120.
42. Even-Sapir E, Metser U, Flusser G, Zuriel L, Kollender Y, Lerman H, et al. Assessment of malignant skeletal disease: initial experience with 18F-fluoride PET/CT and comparison between 18F-fluoride PET and 18F-fluoride PET/CT. J Nucl Med. 2004;45:272–8.
43. Schirrmeister H, Guhlmann A, Elsner K, Kotzerke J, Glatting G, Rentschler M, et al. Sensitivity in detecting osseous lesions depends on anatomic localization: planar bone scintigraphy versus 18F PET. J Nucl Med. 1999;40:1623–9.
44. Schirrmeister H, Glatting G, Hetzel J, Nussle K, Arslandemir C, Buck AK, et al. Prospective evaluation of the clinical value of planar bone scans, SPECT, and (18)F-labeled NaF PET in newly diagnosed lung cancer. J Nucl Med. 2001;42:1800–4.
45. Hetzel M, Arslandemir C, Konig HH, Buck AK, Nussle K, Glatting G, et al. F-18 NaF PET for detection of bone metastases in lung cancer: accuracy, cost-effectiveness, and impact on patient management. J Bone Miner Res. 2003;18:2206–14. doi:10.1359/jbmr.2003.18.12.2206.
46. Drubach LA. Clinical Utility of 18F NaF PET/CT in Benign and Malignant Disorders. Pet Clin. 2012;7:293–301.
47. Uchida K, Nakajima H, Miyazaki T, Yayama T, Kawahara H, Kobayashi S, et al. Effects of alendronate on bone metabolism in glucocorticoid-induced osteoporosis measured by 18F-fluoride PET: a prospective study. J Nucl Med. 2009;50:1808–14. doi:10.2967/jnumed.109.062570.
48. Lim R, Fahey FH, Drubach LA, Connolly LP, Treves ST. Early experience with fluorine-18 sodium fluoride bone PET in young patients with back pain. J Pediatr Orthop. 2007;27:277–82. doi:10.1097/BPO.0b013e31803409ba.
49. Tan AL, Tanner SF, Waller ML, Hensor EM, Burns A, Jeavons AP, et al. High-resolution [18F]fluoride positron emission tomography of the distal interphalangeal joint in psoriatic arthritis—a bone-enthesis-nail complex. Rheumatology. 2013;52:898–904. doi:10.1093/rheumatology/kes384.
50. Strobel K, Fischer DR, Tamborrini G, Kyburz D, Stumpe KD, Hesselmann RG, et al. 18F-fluoride PET/CT for detection of sacroiliitis in ankylosing spondylitis. Eur J Nucl Med Mol Imaging. 2010;37:1760–5. doi:10.1007/s00259-010-1464-7.
51. Kobayashi N, Inaba Y, Tateishi U, Yukizawa Y, Ike H, Inoue T, et al. New application of 18F-fluoride PET for the detection of bone remodeling in early-stage osteoarthritis of the hip. Clin Nucl Med. 2013;38:e379–83. doi:10.1097/RLU.0b013e31828d30c0.
52. Dasa V, Adbel-Nabi H, Anders MJ, Mihalko WM. F-18 fluoride positron emission tomography of the hip for osteonecrosis. Clin Orthop Relat Res. 2008;466:1081–6. doi:10.1007/s11999-008-0219-2.
53. Aratake M, Yoshifumi T, Takahashi A, Takeuchi R, Inoue T, Saito T. Evaluation of lesion in a spontaneous osteonecrosis of the knee using 18F-fluoride positron emission tomography. Knee Surg Sports Traumatol Arthrosc. 2009;17:53–9. doi:10.1007/s00167-008-0641-8.
54. Raje N, Woo SB, Hande K, Yap JT, Richardson PG, Vallet S, et al. Clinical, radiographic, and biochemical characterization of multiple myeloma patients with osteonecrosis of the jaw. Clin Cancer Res. 2008;14:2387–95. doi:10.1158/1078-0432.CCR-07-1430.
55. Wilde F, Steinhoff K, Frerich B, Schulz T, Winter K, Hemprich A, et al. Positron-emission tomography imaging in the diagnosis of bisphosphonate-related osteonecrosis of the jaw. Oral Surg Oral Med Oral Pathol Oral Radiol Endod. 2009;107:412–9. doi:10.1016/j.tripleo.2008.09.019.
56. Installe J, Nzeusseu A, Bol A, Depresseux G, Devogelaer JP, Lonneux M. (18)F-fluoride PET for monitoring therapeutic response in Paget's disease of bone. J Nucl Med. 2005;46:1650–8.
57. Fischer DR, Maquieira GJ, Espinosa N, Zanetti M, Hesselmann R, Johayem A, et al. Therapeutic impact of [(18)F]fluoride positron-emission tomography/computed tomography on patients with unclear foot pain. Skelet Radiol. 2010;39:987–97. doi:10.1007/s00256-010-0875-7.
58. Sterner T, Pink R, Freudenberg L, Jentzen T, Quitmann H, Bockisch A, et al. The role of [18F]fluoride positron emission tomography in the early detection of aseptic loosening of total knee arthroplasty. Int J Surg. 2007;5:99–104. doi:10.1016/j.ijsu.2006.05.002.
59. Temmerman OP, Raijmakers PG, Heyligers IC, Comans EF, Lubberink M, Teule GJ, et al. Bone metabolism after total hip revision surgery with impacted grafting: evaluation using H2 15O and [18F]fluoride PET; a pilot study. Mol Imaging Biol. 2008;10:288–93. doi:10.1007/s11307-008-0153-4.
60. Slipman CW, Patel RK, Vresilovic EJ, Brautigam P, Mathies A, Adam LE, et al. Osseous stress reaction in a rower diagnosed with positron emission tomography (PET): a case report. Pain Phys. 2001;4:336–42.
61. Berding G, Burchert W, van den Hoff J, Pytlik C, Neukam FW, Meyer GJ, et al. Evaluation of the incorporation of bone grafts used in maxillofacial surgery with [18F]fluoride ion and dynamic positron emission tomography. Eur J Nucl Med. 1995;22:1133–40.
62. Brenner W, Bohuslavizki KH, Eary JF. PET imaging of osteosarcoma. J Nucl Med. 2003;44:930–42.
63. Drubach LA, Johnston PR, Newton AW, Perez-Rossello JM, Grant FD, Kleinman PK. Skeletal trauma in child abuse: detection with 18F-NaF PET. Radiology. 255:173–81. doi: 10.1148/radiol.09091368.
64. Ovadia D, Metser U, Lievshitz G, Yaniv M, Wientroub S, Even-Sapir E. Back pain in adolescents: assessment with integrated 18F-fluoride positron-emission tomography-computed tomography. J Pediatr Orthop. 2007;27:90–3. doi:10.1097/01.bpo.0000242438.11682.10.
65. Laverick S, Bounds G, Wong WL. [18F]-fluoride positron emission tomography for imaging condylar hyperplasia. Br J Oral Maxillofac Surg. 2009;47:196–9. doi:10.1016/j.bjoms.2008.08.001.
66. Donohoe KJ, Henkin RE, Royal HD, Brown ML, Collier BD, O'Mara RE, et al. Procedure guideline for bone scintigraphy: 1.0. Society of Nuclear Medicine. J Nucl Med. 1996;37:1903–6.
67. Treves ST, Parisi MT, Gelfand MJ. Pediatric radiopharmaceutical doses: new guidelines. Radiology. 261:347–9. doi: 10.1148/radiol.11110449.
68. Blau M, Ganatra R, Bender MA. 18 F-fluoride for bone imaging. Semin Nucl Med. 1972;2:31–7.
69. Hoegerle S, Juengling F, Otte A, Altehoefer C, Moser EA, Nitzsche EU. Combined FDG and [F-18]fluoride whole-body PET: a feasible two-in-one approach to cancer imaging? Radiology. 1998;209:253–8.
70. Brunkhorst T, Boerner AR, Bergh S, Otto D, Gratz FW, Knapp WH. Pretherapeutic assessment of tumour metabolism using a dual tracer PET technique. Eur J Nucl Med Mol Imaging. 2002;29:1416. doi:10.1007/s00259-002-0964-5.

71. Iagaru A, Mittra E, Yaghoubi SS, Dick DW, Quon A, Goris ML, et al. Novel strategy for a cocktail 18F-fluoride and 18F-FDG PET/CT scan for evaluation of malignancy: results of the pilot-phase study. J Nucl Med. 2009;50:501–5. doi:10.2967/jnumed.108.058339.
72. Frost ML, Cook GJ, Blake GM, Marsden PK, Benatar NA, Fogelman I. A prospective study of risedronate on regional bone metabolism and blood flow at the lumbar spine measured by 18F-fluoride positron emission tomography. J Bone Miner Res. 2003;18:2215–22. doi:10.1359/jbmr.2003.18.12.2215.
73. Frost ML, Siddique M, Blake GM, Moore AE, Schleyer PJ, Dunn JT, et al. Differential effects of teriparatide on regional bone formation using (18)F-fluoride positron emission tomography. J Bone Miner Res. 26:1002–11. doi:10.1002/jbmr.305.
74. Schiepers C, Nuyts J, Bormans G, Dequeker J, Bouillon R, Mortelmans L, et al. Fluoride kinetics of the axial skeleton measured in vivo with fluorine-18-fluoride PET. J Nucl Med. 1997;38:1970–6.
75. Cook GJ, Lodge MA, Marsden PK, Dynes A, Fogelman I. Non-invasive assessment of skeletal kinetics using fluorine-18 fluoride positron emission tomography: evaluation of image and population-derived arterial input functions. Eur J Nucl Med. 1999;26:1424–9.
76. Blake GM, Seddique M, Frost ML, Moore AE, Fogelman I. Quantitative PET imaging using 18F Sodium Fluoride in the assessment of metabolic bone disease and the monitoting of their response to therapy. Pet Clin. 2012;7:275–91.
77. Wootton R, Dore C. The single-passage extraction of 18F in rabbit bone. Clin Phys Physiol Meas. 1986;7:333–43.
78. Piert M, Zittel TT, Machulla HJ, Becker GA, Jahn M, Maier G, et al. Blood flow measurements with [(15)O]H2O and [18F]fluoride ion PET in porcine vertebrae. J Bone Miner Res. 1998;13:1328–36. doi:10.1359/jbmr.1998.13.8.1328.
79. Siddique M, Blake GM, Frost ML, Moore AE, Puri T, Marsden PK, et al. Estimation of regional bone metabolism from whole-body 18F-fluoride PET static images. Eur J Nucl Med Mol Imaging. 39:337–43. doi:10.1007/s00259-011-1966-y.
80. Blake GM, Siddique M, Frost ML, Moore AE, Fogelman I. Radionuclide studies of bone metabolism: do bone uptake and bone plasma clearance provide equivalent measurements of bone turnover? Bone. 49:537–42. doi: 10.1016/j.bone.2011.05.031.
81. Kawaguchi M, Tateishi U, Shizukuishi K, Suzuki A, Inoue T. 18F-fluoride uptake in bone metastasis: morphologic and metabolic analysis on integrated PET/CT. Ann Nucl Med. 2010;24:241–7. doi:10.1007/s12149-010-0363-0.
82. Vali R, Beheshti M, Waldenberger P, Fitz F, Haim S, Nader M, et al. Assessment of malignant and benighn bone lesions by static F-18 Fluoride PET-CT: additional value of SUV! J Nucl Med. 2008;49:150P.
83. Cook Jr G, Parker C, Chua S, Johnson B, Aksnes AK, Lewington VJ. 18F-fluoride PET: changes in uptake as a method to assess response in bone metastases from castrate-resistant prostate cancer patients treated with 223Ra-chloride (Alpharadin). EJNMMI Res. 2011;1:4. doi:10.1186/2191-219X-1-4.
84. Tateishi U, Morita S, Taguri M, Shizukuishi K, Minamimoto R, Kawaguchi M, et al. A meta-analysis of (18)F-Fluoride positron emission tomography for assessment of metastatic bone tumor. Ann Nucl Med. 24:523–31. doi:10.1007/s12149-010-0393-7.
85. Xia T, Alessio AM, De Man B, Manjeshwar R, Asma E, Kinahan PE. Ultra-low dose CT attenuation correction for PET/CT. Phys Med Biol. 57:309–28. doi:10.1088/0031-9155/57/2/309.
86. Huang B, Law MW, Khong PL. Whole-body PET/CT scanning: estimation of radiation dose and cancer risk. Radiology. 2009;251:166–74. doi:10.1148/radiol.2511081300.
87. Beheshti M, Vali R, Waldenberger P, Fitz F, Nader M, Loidl W, et al. Detection of bone metastases in patients with prostate cancer by 18F fluorocholine and 18F fluoride PET-CT: a comparative study. Eur J Nucl Med Mol Imaging. 2008;35:1766–74. doi:10.1007/s00259-008-0788-z.
88. Radiation dose to patients from radiopharmaceuticals (addendum 3 to ICRP Publication 53) ICRP publication 106 approved by the Commission in October 2007. Ann ICRP 2008;38:1–197.
89. Radiation dose to patients from radiopharmaceuticals (addendum 2 to ICRP publication 53): ICRP publication 80, approved by the Commission in September 1997. Ann ICRP. 1998;28:1–126.